

A geometrically-based mean-field theory of polydisperse hard-sphere mixtures

P. Bartlett

School of Chemistry, University of Bath, Claverton Down, Bath BA2 7AY, United Kingdom

(Received 30 October 1996; accepted 28 March 1997)

We present a mean-field description of a system of polydisperse hard-spheres. The theory is based on the postulate that the excess statistical properties of a general polydisperse mixture are a function of the number, the mean diameter, surface area, and volume of the constituent particles. Within this model a corresponding states relationship holds between a general polydisperse system and a suitably chosen two-component mixture. This equivalence is used to derive approximate expressions for the free energy and pressure of polydisperse crystal and fluid phases. Quantitative results are presented for the case of a Schultz distribution of diameters. These free energies are used to calculate the solid–fluid phase diagram as a function of diameter polydispersity. We find a terminal polydispersity of 8.3% above which the polydisperse fluid remains stable at all densities. In contrast with recent simulations we find no evidence for a substantial fractionation in diameters between the coexisting fluid and solid phases. © 1997 American Institute of Physics. [S0021-9606(97)51325-0]

I. INTRODUCTION

In the last decade considerable progress has made in understanding the rich and varied phase behavior of colloidal suspensions.^{1,2} One of the most fruitful ideas has proved to be the analogy between colloids and simple atomic systems.³ At least in a formal sense the equilibrium statistical mechanics of a suspension of *uniform* colloidal particles is identical with that of an atomic system interacting with the same potential. This link has meant that the techniques and concepts of classical statistical mechanics have been utilized extensively to understand the rich statistical phenomena observed in colloidal systems. This is most evident in the case of “hard sphere” colloids where considerable experimental and theoretical effort has established a remarkably exotic set of phase behavior.^{4–7} Indeed the hard core system plays a crucial role in colloid physics because, as for simple fluids, the microscopic structure of suspensions is dominated by short-range repulsive interactions; longer-range attractions contribute to thermodynamics only in a mean-field approximation.

There is, however, one important aspect in which colloids and atoms differ. While all atoms of the same element are identical in size there is inevitably a distribution of sizes among the components of any colloidal suspension. This diameter variation or “polydispersity” is unavoidable in any experimental system. Indeed considerable experimental effort is normally necessary to reduce the diameter variation to a level at which an approximation by identically sized particles is realistic. While it is clear that, in principle, polydispersity could modify the thermodynamic properties of suspensions, shift phase transitions or even in extreme cases prevent them from occurring there is, as yet, an incomplete understanding of the role of polydispersity. In the main this is because of the lack of simple accurate statistical models of colloidal systems with a continuous distribution of diameters. The purpose of this paper is to demonstrate a general geometric equivalence between a polydisperse mixture and a

binary hard-sphere system. Since the properties of binary mixtures are much more amenable to analysis this equivalence allows the properties of polydisperse systems to be readily approximated. To test the accuracy of our approach we calculate the influence of polydispersity on the fluid–solid phase boundaries in hard spheres.

The influence of polydispersity on the fluid–solid phase transition of hard spheres was first examined by Dickinson and Parker⁸ who found that the width of the coexistence region narrows as polydispersity increases. They suggested that above a terminal polydispersity of about 11% (defined as the standard deviation of the diameter distribution divided by the mean diameter) the transition should disappear entirely. Similar conclusions were reached using density functional arguments^{9,10} although the terminal polydispersity was estimated as being between 5% and 7%. The problem has been reexamined recently¹¹ by computer simulation. A polydisperse system was simulated by *imposing* a Gaussian chemical potential distribution. The identity of each particle was then allowed to change so as to simulate, at equilibrium, a continuous diameter distribution. While the results, from this study, for the terminal polydispersity were broadly in line with previous estimates the authors found a significant degree of fractionation between the coexisting fluid and solid phases. The diameter distribution in the fluid phase was peaked around a lower mean diameter and was considerably broader than the distribution found in the coexisting solid phase.

In this paper we report a mean-field treatment of polydispersity in hard-sphere mixtures. The theory is formulated in Sec. II. In Sec. II A we apply this method to calculate the pressure and free energy of a polydisperse solid solution while the thermodynamics of the polydisperse fluid phase are described in Sec. II B. The theory of the solid–fluid phase coexistence in a polydisperse hard-sphere mixture is outlined

in Sec. III, followed by a description of our main results in Sec. IV.

II. METHOD

To compute the fluid–solid coexistence in a polydisperse hard-sphere mixture we use a geometric mean-field approach inspired by scaled particle theory^{12,13} (SPT). The SPT has been applied previously, to the best of our knowledge, only to fluid systems. We assume here that the underlying geometric ideas are applicable equally to solids as to fluids. Below we outline the basis of our approach. In a later section we apply the theory to calculate the equation of state of a polydisperse hard-sphere crystal.

Consider a polydisperse system of hard spheres in which the scaled sphere diameter $\alpha = R/\bar{R}$, where \bar{R} is the mean diameter, is distributed according to the normalized density function $f(\alpha)$. The probability of finding a sphere with a scaled diameter between α and $\alpha + d\alpha$ is therefore $f(\alpha)d\alpha$. Let $\rho = N/V$ be the total number of particles per unit volume. For convenience we introduce the following moments of the diameter distribution

$$\xi_j = \frac{\pi}{6} \rho \bar{R}^j \int_0^\infty \alpha^j f(\alpha) d\alpha. \quad (1)$$

The zeroth and first moments define the number density and mean diameter

$$\rho = \frac{6}{\pi} \xi_0, \quad \bar{R} = \frac{6}{\pi \rho} \xi_1. \quad (2)$$

While σ , the relative standard deviation of the diameter distribution or *polydispersity*

$$\sigma^2 = \frac{\overline{R^2}}{\bar{R}^2} - 1, \quad (3)$$

is related to the second moment by

$$\xi_2 = \frac{\pi}{6} \rho \bar{R}^2 (1 + \sigma^2). \quad (4)$$

The third moment ξ_3 is simply the total hard-sphere volume fraction ϕ .

The starting point for our approach is an expression for the excess chemical potential $\mu^{\text{ex}}(\alpha)$ of the species of diameter α in the polydisperse system. Our basic approximation is that $\mu^{\text{ex}}(\alpha)$ is given by a cubic polynomial for all α of the form

$$\beta \mu^{\text{ex}}(\alpha) = D\alpha^3 + C\alpha^2 + B\alpha + A, \quad (5)$$

where $\beta = 1/k_B T$ and A , B , C , and D are coefficients which depend on ϕ and the function $f(\alpha)$. We derive expressions for A and D below.

This expression has been discussed in earlier work^{12,13} on the application of scaled particle theory to fluids but we repeat the justification of Eq. (5) here for clarity. The excess chemical potential $\mu^{\text{ex}}(\alpha)$ may be identified formally with the work of inserting, at some fixed position \mathbf{R} in the system, a *single* hard-sphere particle of diameter α . Inserting a hard-

sphere particle at \mathbf{R} excludes the centers of all neighboring species with a diameter α_i from a spherical region of diameter $\alpha + \alpha_i$ about \mathbf{R} . For $\alpha \geq 0$ this is equivalent to excluding *any* part of a neighboring particle from a region of diameter α centered on \mathbf{R} and consequently the addition is equivalent to creating a cavity of diameter α . $\mu^{\text{ex}}(\alpha)$ is therefore equal to the reversible work expended in making a cavity of diameter α . While in general the function $\mu^{\text{ex}}(\alpha)$ is unknown, we approximate it by appealing to its limiting form at small and large α .

The excess chemical potential of a point particle is readily calculated from the Widom insertion expression.¹⁴ The probability of inserting a point particle into a system of hard spheres of volume fraction ϕ is proportional to $1 - \phi$. Consequently the excess chemical potential, in the limit of $\alpha = 0$, is exactly

$$\lim_{\alpha \rightarrow 0} \beta \mu^{\text{ex}}(\alpha) = -\ln(1 - \phi). \quad (6)$$

Consider now the case of α very large. The leading term in $\beta \mu^{\text{ex}}(\alpha)$ is the pressure-volume work required to exclude particles from a cavity of diameter α . If P is the pressure of the hard-sphere system, then the leading term to the chemical potential is the cubic contribution $(\pi/6) \beta P \bar{R}^3 \alpha^3$. There is also a contribution from the surface energy of the cavity which will be quadratic in α . This is of the form $4\pi \bar{R}^2 \beta \gamma_\alpha \alpha^2$, where γ_α is the surface tension of a spherical cavity of diameter α . Taking into account the curvature dependence¹⁵ of the surface tension

$$\gamma_\alpha = \gamma_0 \left(1 - \frac{\delta}{\alpha \bar{R}} \right) \quad (7)$$

results in a further linear contribution to $\beta \mu^{\text{ex}}(\alpha)$. Here δ is a length of order \bar{R} and γ_0 is the surface tension of the cavity in the limit of $\alpha \rightarrow \infty$. Combining these terms with the $\alpha = 0$ limit gives an expression of the form

$$\beta \mu^{\text{ex}}(\alpha) = \frac{\pi}{6} \beta P \bar{R}^3 \alpha^3 + C\alpha^2 + B\alpha - \ln(1 - \phi), \quad (8)$$

where the coefficients B and C are functions of ϕ and, in general, functionals of the diameter distribution $f(\alpha)$. Although the form of Eq. (8) has been derived from macroscopic arguments the success of SPT suggests that this expression can be successfully extrapolated to particle dimensions, at least for fluids.¹⁶ We assume that similar considerations hold for the solid phase.

The total chemical potential, $\mu(\alpha)$, of the species of diameter α is the sum of the excess component [given by Eq. (8)] and an ideal contribution,¹⁷ $\beta \mu^{\text{id}}(\alpha) = \ln \rho \Lambda^3(\alpha) f(\alpha)$, where $\Lambda(\alpha)$ is the thermal wavelength of the species with diameter α . To calculate the pressure of the polydisperse system we use the thermodynamic relation,

$$\left(\frac{\partial P}{\partial \rho_j} \right)_T = \sum_i \rho_i \left(\frac{\partial \mu_i}{\partial \rho_j} \right)_T, \quad (9)$$

or rather its generalization to a continuous distribution,

TABLE I. A binary mixture of hard spheres with a fixed value for the total number density of particles of ρ_b and a mean diameter of \bar{R}_b . The properties of the mixture are a function of the variables δ and Δ .

	Large species	Small species
Number density	$\rho_b \frac{(1-\Delta)}{2}$	$\rho_b \frac{(1+\Delta)}{2}$
Diameter	$\bar{R}_b \frac{(1+\delta)}{(1-\Delta)}$	$\bar{R}_b \frac{(1-\delta)}{(1+\Delta)}$

$$\left(\frac{\partial P}{\partial [f]} \right)_T = \rho \int_0^\infty f(\alpha) \left(\frac{\partial \mu}{\partial [f]} \right)_T d\alpha, \quad (10)$$

where $\partial P / \partial [f]$ is the functional derivative of P . It is apparent from above that if $\mu^{ex}(\alpha)$ is a cubic polynomial in α , then the pressure P must be a function of, at least, the first four moments of the diameter distribution (ξ_j , $j=0, \dots, 3$). Substitution of Eq. (8) into Eq. (10) and integration demonstrates that a dependence of the pressure upon moments higher than ξ_3 arises *only* if the coefficients B or C depend themselves upon such moments. To proceed we make the simplest hypothesis, consistent with the form assumed in Eq. (8), that the pressure P and the excess chemical potential are functions *only* of the first four moments so Eq. (8) becomes

$$\beta \mu^{ex}(\alpha) = \frac{\pi}{6} \beta P(\xi_0, \xi_1, \xi_2, \xi_3) \bar{R}^3 \alpha^3 + C(\xi_0, \xi_1, \xi_2, \xi_3) \alpha^2 + B(\xi_0, \xi_1, \xi_2, \xi_3) \alpha - \ln(1 - \phi). \quad (11)$$

While the discussion above is little more than suggestive, the idea that the statistical mechanics of a polydisperse system of hard spheres is a function of such basic geometric variables as the total number, mean size, surface area, and volume of particles is very appealing physically. Furthermore it suggests that it is feasible to approximate the properties of a polydisperse system by a limited set of discrete components. In particular the pressure and the excess chemical potential of a polydisperse and an equivalent discrete system will be identical provided that

$$\xi_j = \xi_j(\text{discrete}) \quad \text{for } j=0, \dots, 3. \quad (12)$$

Rather surprisingly, to match the first four moments of any diameter distribution requires, in general, only two differently sized components. To see this consider the binary distribution detailed in Table I. This distribution has been chosen so that varying δ and Δ allow the mixture composition and volume fraction to change while the total number density and mean diameter are fixed at ρ_b and \bar{R}_b , respectively. The first four diameter moments of the binary mixture are readily calculated as

$$\begin{aligned} \xi_0(\text{binary}) &= \frac{\pi}{6} \rho_b, \\ \xi_1(\text{binary}) &= \frac{\pi}{6} \rho_b \bar{R}_b, \\ \xi_2(\text{binary}) &= \frac{\pi}{12} \rho_b \bar{R}_b^2 \left\{ \frac{(1-\delta)^2}{1+\Delta} + \frac{(1+\delta)^2}{1-\Delta} \right\}, \\ \xi_3(\text{binary}) &= \frac{\pi}{12} \rho_b \bar{R}_b^3 \left\{ \frac{(1-\delta)^3}{(1+\Delta)^2} + \frac{(1+\delta)^3}{(1-\Delta)^2} \right\}. \end{aligned} \quad (13)$$

The zeroth and first moment of the binary and polydisperse mixture are matched by simply equating the number density ($\rho_b = \rho$) and the mean particle diameter ($\bar{R}_b = \bar{R}$) of the two distributions. Equating the remaining two moments of the polydisperse mixture gives a pair of simultaneous conditions on the binary variables δ and Δ . Solving these two equations fixes the composition and density of the binary mixture which is a corresponding state model for the polydisperse system.

To obtain quantitative results it is necessary to consider a particular probability density function. For computational ease we consider only the Schultz (or generalized exponential) distribution

$$f(\alpha) = \frac{(z+1)^{z+1}}{z!} \alpha^z \exp[-(z+1)\alpha], \quad (14)$$

where the polydispersity σ is related to the parameter z by

$$\sigma^2 = \frac{1}{z+1}. \quad (15)$$

The moments of the Schultz distribution may be calculated analytically with the results

$$\begin{aligned} \xi_j &= \frac{\pi}{6} \rho \bar{R}^j \frac{(z+j)!}{z!(z+1)^j} \\ &= \frac{\pi}{6} \rho \bar{R}^j [1 + (j-1)\sigma^2][1 + (j-2)\sigma^2] \cdots [1 + \sigma^2]. \end{aligned} \quad (16)$$

Equating the first four moments gives the parameters of the equivalent binary distribution. The binary mixture equivalent to a Schultz-distributed polydisperse system of number density ρ , mean diameter \bar{R} , and polydispersity σ is

$$\begin{aligned} \rho_b &= \rho, \quad \bar{R}_b = \bar{R}, \\ \Delta^2 &= \frac{\sigma^2}{1 + \sigma^2}, \quad \delta = 0. \end{aligned} \quad (17)$$

Since this distribution matches exactly the first four moments of the Schultz system a natural question is the accuracy of higher moments. The moments of the equivalent binary distribution, from Eq. (17), are

$$\xi_j = \frac{\pi}{12} \rho \bar{R}^j \left\{ \frac{1}{(1+\Delta)^{j-1}} + \frac{1}{(1-\Delta)^{j-1}} \right\}, \quad (18)$$

which in the limit of small polydispersity may be approximated as

$$\xi_j = \frac{\pi}{6} \rho \bar{R}^j \left[1 + \frac{j(j-1)}{2} \sigma^2 + O(\sigma^4) \right]. \quad (19)$$

Inspection shows that these values are identical with the moments of the Schultz distribution to terms of order σ^2 . Consequently while the higher moments, ξ_j with $j > 3$, of the Schultz and binary distributions are in general different, in the limit of small polydispersity *all* moments of the binary and Schultz distributions are equal.

Our general approach should now be clear. We assume that the excess thermodynamic properties of a polydisperse system are functions only of the first four moments of the diameter distribution. To approximate the polydisperse mixture we consider the equivalent binary system described in Table I and Eq. (17). Equating the excess thermodynamic properties of the two corresponding systems gives the excess chemical potential of the polydisperse system at *all* diameters from Eq. (11).

A. Polydisperse crystal

To illustrate how the ideas of the last section may be applied we now calculate the thermodynamic properties of a Schultz-distributed polydisperse FCC crystal. The equivalent binary system is the substitutionally disordered FCC hard-sphere crystal (a solid solution) which has been studied extensively by Kranendonk and Frenkel^{18–20} using computer simulation techniques. In this study the authors studied binary hard-sphere mixtures of diameter ratios $\alpha = 0.95, 0.90$, and 0.85 . Both the equation of state and the excess free energies of the binary substitutional crystals were determined. Conveniently for the present discussion, the authors express their simulation data in terms of a set of symmetry-adapted analytical functions for the pressure and excess free energy. It is then straightforward to evaluate the excess chemical potential of the large (μ_L^{ex}) and small spheres (μ_S^{ex}) in terms of the ratio R_S/R_L of the diameters of the small and large spheres, the composition X_L defined as the mole ratio of large spheres and the volume fraction ϕ_b of the binary crystal.

To discuss the thermodynamics of the polydisperse crystal we use as variables the volume fraction ϕ , the mean diameter \bar{R} , and the polydispersity σ of the diameter distribution rather than the moments, ξ_j . For a Schultz distribution the two sets of variables are readily related from Eq. (16). Inspection of Eq. (17) shows that the equivalent binary mixture has a volume fraction of ϕ , a diameter ratio of $R_S/R_L = (1 - \Delta)/(1 + \Delta)$, and a composition $X_L = (1 - \Delta)/2$ where $\Delta = \sigma/\sqrt{1 + \sigma^2}$. The pressure of the binary solid is readily obtained from the analytical expressions given by Kranendonk and Frenkel.²⁰ We find that the pressure of the polydisperse solid is always *higher* than the pressure of the monodisperse system of the same volume fraction. This is illustrated in Fig. 1 where the reduced pressure ($\beta P \bar{R}^3$) of the solid is plotted versus the polydispersity at a fixed volume fraction of $\phi = 0.545$. On a qualitative level the increase

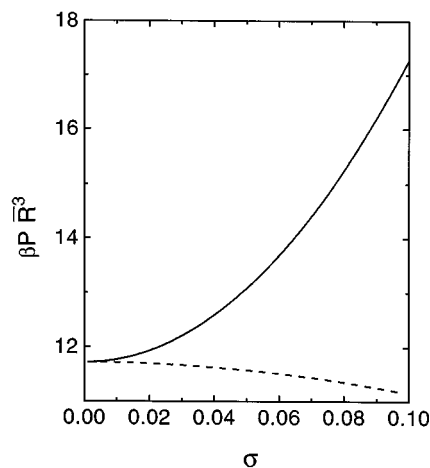


FIG. 1. Reduced pressure $\beta P \bar{R}^3$ as a function of the normalized width σ of the Schultz distribution of diameters. Results for a polydisperse solid (solid line) with a fixed volume fraction of $\phi = 0.545$ and a polydisperse fluid (dashed line) of volume fraction $\phi = 0.493$ are shown.

in pressure with polydispersity reflects the reduction in free volume as it becomes increasingly difficult to efficiently pack very different-sized spheres in a unit cell without distorting the cell.

The accuracy of the mean-field approximation may be assessed by a comparison with the simulation results obtained by Bolhuis and Kofke.¹¹ Unfortunately an unambiguous test is difficult because the diameter distribution in the simulation was not fixed but varied as a result of the fixed chemical potential distribution assumed. However, for narrow distributions, we expect that the key property of a distribution is its width rather than detailed shape. This is certainly the case within the current theory where polydisperse systems with different diameter distributions have very similar statistical properties *when compared at fixed* σ . Consequently, to a first approximation, it is not necessary to know the detailed form of the diameter distribution used in the simulation. The simulation results may be compared directly with a calculation, for example, of a Schultz-distributed solid of the *same* polydispersity. Figure 2 shows such a comparison between the present theory (solid line) and the simulation data of Bolhuis and Kofke¹¹ (circles) for the pressure of the polydisperse solid. The reduced pressure, $\beta P \bar{R}^3$, is plotted as a function of the diameter polydispersity along the fluid–solid coexistence line determined by Bolhuis and Kofke. The inset plot in Fig. 2 gives the volume fraction of the solid phase along the same coexistence line. As can be seen from Fig. 2 the agreement between theory and simulation is reasonably good although at high polydispersities and high densities the mean-field theory does seem to overestimate slightly the pressure.

The diameter dependence of the excess chemical potential in the polydisperse solid may be obtained from Eq. (11) and the values for the chemical potentials in the (equivalent) binary system, μ_L^{ex} and μ_S^{ex} . The normalized diameters (scaled by \bar{R}) of the large and small species in the equivalent binary mixture are, from Table I,

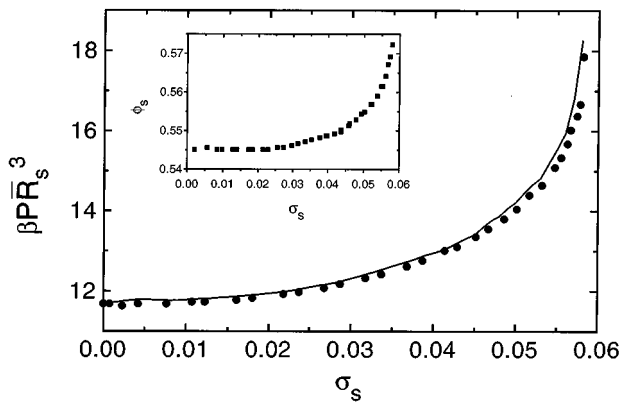


FIG. 2. The pressure of the polydisperse solid as a function of the diameter distribution width σ_s . The volume fraction of the solid, at each value of σ_s , is fixed at the coexisting solid density determined by Bolhuis and Kofke (Ref. 11). The inset graph shows the resulting volume fraction, ϕ_s , as a function of σ_s . The solid line depicts the results of the mean-field approximation for a Schultz diameter distribution while the computer simulation results (Ref. 11) are shown as points.

$$\alpha_L = \frac{1}{1 - \Delta} \quad (20)$$

$$\alpha_S = \frac{1}{1 + \Delta}.$$

From the arguments above, for these two diameters, the excess chemical potential of the polydisperse system and the corresponding binary mixture are equal. Substitution in Eq. (11) gives two simultaneous equations, at $\alpha = \alpha_L$ and α_S , which may be solved to give the undetermined coefficients B and C at each value of (ϕ, σ, \bar{R}) . Figure 3 illustrates the dependence of the excess chemical potential in the solid phase on polydispersity. The calculations are for a fixed volume fraction of $\phi = 0.545$ and refer to the particle of mean diameter \bar{R} . It is evident from this figure that the influence of increased polydispersity is to destabilize the solid phase.

B. Polydisperse fluid

In the case of a fluid phase the arguments outlined in Sec. II are identical with the starting point of the conventional scaled particle theory (SPT) of hard sphere mixtures. In the original derivation of Reiss *et al.* the unknown coefficients in the expression for the excess chemical potential [Eq. (8)] were determined¹² by ensuring essentially that the first and second derivative of $\mu^{\text{ex}}(R)$ were continuous at $R=0$.

The excess chemical potential from SPT of the species of diameter R in a polydisperse fluid, namely

$$\beta \mu_{\text{SPT}}^{\text{ex}}(R) = \frac{\pi}{6} \beta P_{\text{SPT}} R^3 + \frac{9\xi_2^2 - 6\xi_1\xi_3 + 6\xi_1}{2(1 - \xi_3)^2} R^2 + \frac{3\xi_2}{(1 - \xi_3)} R - \ln(1 - \xi_3), \quad (21)$$

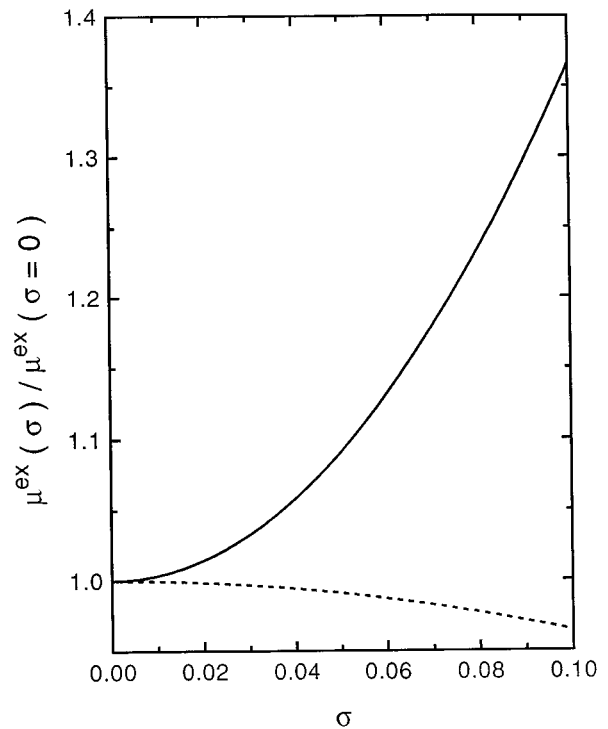


FIG. 3. The excess chemical potential (normalized by the monodisperse value) as a function of the polydispersity σ of the diameter distribution. The solid line depicts the chemical potential of the particle of mean diameter in a polydisperse solid of fixed volume fraction $\phi = 0.545$. The dashed line refers to the polydisperse fluid of volume fraction $\phi = 0.493$.

can be obtained, formally, from the SPT results derived for a binary hard-sphere fluid¹³ using the approach discussed in the previous section. As expected the form predicted by scaled particle theory is consistent with the general polydisperse expression given in Eq. (11).

Here we choose not to use the SPT result for numerical calculations since computer simulations of mixtures show small but significant deviations from SPT. For a binary mixture of hard spheres the Mansoori, Carnahan, Starling, and Leland (MCSL) equation of state,²¹ which is simply a weighted average of the Percus–Yevick (PY) compressibility (which is identical with the SPT result) and virial pressures

$$\beta P_{\text{Man}} = \frac{2}{3} \beta P_c + \frac{1}{3} \beta P_v, \quad (22)$$

yields results which are in much closer agreement with simulation.²⁰ We therefore choose a polydisperse MCSL equation rather than the SPT result to approximate the polydisperse fluid phase. For a polydisperse system the MCSL approximation has been written as¹⁷

$$\beta P_{\text{Man}} = \frac{6}{\pi} \left\{ \frac{\xi_0}{1 - \xi_3} + \frac{3\xi_1\xi_2}{(1 - \xi_3)^2} + \frac{3\xi_2^3 - \xi_3\xi_2^3}{(1 - \xi_3)^3} \right\}. \quad (23)$$

Standard manipulation gives the following expression for the excess chemical potential:

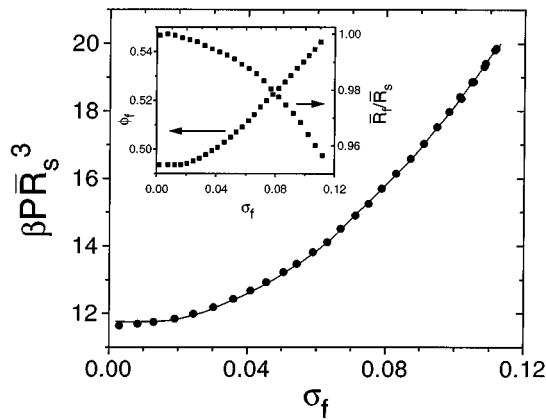


FIG. 4. The reduced pressure of a polydisperse fluid as a function of the width of the diameter distribution. The solid line represents the Mansoori approximation for a Schultz distribution. The computer simulation results of Bolhuis and Kofke (Ref. 11) are denoted by the filled circles. The volume fraction (ϕ_f) and mean diameter (R_f/R_s) are fixed at the coexisting fluid values determined by Bolhuis and Kofke and are shown in the inset plot.

$$\begin{aligned} \beta \mu_{\text{Man}}^{\text{ex}}(R) = R^3 & \left\{ \frac{\pi}{6} \beta P_{\text{Man}} + \frac{\xi_2^3(\xi_3 - 2)}{\xi_3^2(1 - \xi_3)} \right. \\ & \left. - 2 \left(\frac{\xi_2}{\xi_3} \right)^3 \ln(1 - \xi_3) \right\} \\ & + R^2 \left\{ \frac{3\xi_1}{1 - \xi_3} + \frac{3\xi_2^2}{\xi_3^2(1 - \xi_3)^2} \right. \\ & \left. + 3 \left(\frac{\xi_2}{\xi_3} \right)^2 \ln(1 - \xi_3) \right\} + \frac{3\xi_2}{1 - \xi_3} R - \ln(1 - \xi_3). \end{aligned} \quad (24)$$

In contrast with the SPT result, this expression is not consistent with the general polydisperse form [Eq. (11)]. The reason for this discrepancy is that the virial form of the Percus–Yevick approximation which is included in the Mansoori average is itself not thermodynamically self-consistent.²² Even with this restriction a comparison with simulation data for polydisperse hard-sphere fluids suggests that the Mansoori equation of state is remarkably reliable.

Figure 4 compares the fluid pressure determined by simulation¹¹ with the results from Eq. (23) calculated for a Schultz-distributed fluid with a diameter polydispersity of σ_f . Simulation data is currently only available for the properties of the *coexisting* polydisperse fluid phase. The corresponding density and mean diameter of the fluid phase, found by simulation,¹¹ are shown in the inset graph. As may be seen the results of the computer simulation are represented very accurately by the Mansoori approximation proposed by Salacuse and Stell.¹⁷

In the limit of small polydispersity the pressure, from the Mansoori expression, for a Schultz-distributed fluid, may be written as

$$P_{\text{Man}} = P_{\text{cs}} \left\{ 1 - 3\sigma^2 \frac{1 + 3\phi + 2\phi^2 - 2\phi^3}{1 + \phi + \phi^2 - \phi^3} + O(\sigma^4) \right\}, \quad (25)$$

where P_{cs} is the Carnahan and Starling result¹⁶ for the pressure of a fluid of monodisperse hard spheres. The pressure of the polydisperse fluid is therefore always *lower* than the monodisperse system at the same total volume fraction in marked contrast with the solid phase. This is illustrated in Fig. 1 where the reduced pressure ($\beta P_{\text{Man}} \bar{R}^3$) is plotted as a function of polydispersity for a Schultz-distributed fluid of fixed volume fraction $\phi = 0.493$. The lower pressure in the polydisperse fluid reflects the increased efficiency of packing and consequent increase in the free volume as smaller particles pack in the cavities between larger particles. The same effect is responsible for the observed decrease in (excess) chemical potential with increasing polydispersity displayed in Fig. 3—increasing mixture polydispersity enhances the stability of the fluid phase.

III. POLYDISPERSE PHASE EQUILIBRIA

The difficulty in calculating phase equilibria in a polydisperse system is that, in general, the diameter distribution will not be the same in the two coexisting phases. If we denote the two coexisting phases²³ by f and s and the corresponding diameter distributions by $f_f(R)$ and $f_s(R)$, then the conditions for equilibrium are, in principle, the infinite set of coupled equations¹⁷

$$\begin{aligned} P_s &= P_f, \\ \mu_s(R) &= \mu_f(R) \quad \text{for } 0 < R < \infty. \end{aligned} \quad (26)$$

These equations must be solved for the two distributions together with the constraint that the total number of particles of diameter R is fixed so that

$$N(R) = N_f f_f(R) + N_s f_s(R), \quad (27)$$

where N_f and N_s are the total number of particles in the coexisting phases. To simplify this problem we assume that both phases may be represented by a Schultz distribution of diameters. To include the possibility that for instance the solid phase will be richer in large particles than the coexisting fluid we allow the mean diameter and polydispersity of the fluid and solid distributions to be, in general, different.

Assuming that the diameter distribution has a simple analytical form reduces dramatically the number of degrees of freedom and considerably simplifies the problem. However, this simplification has two unfortunate consequences. First, in general, it is not possible to satisfy the conservation condition and the conditions for chemical equilibrium simultaneously, and second, the conditions for thermodynamic equilibrium cannot be satisfied for all R .

Here we avoid the difficult task of ensuring that particle numbers are conserved by considering only the marginal stability of the polydisperse solid. That is we seek to find the properties of the polydisperse fluid which is generated as an infinitesimal amount of the solid melts. This occurs as the upper boundary of the region of fluid–solid coexistence is crossed where the system is composed almost entirely of a single phase and the conservation conditions are violated then only infinitesimally.

With the assumption of a Schultz distribution, the phase behavior of the polydisperse mixture is characterized by the volume fractions of the two coexisting phases, ϕ_f and ϕ_s , and the mean diameter and polydispersities of the fluid (\bar{R}_f, σ_f) and solid (\bar{R}_s, σ_s). The problem of determining the stability boundaries of a solid of given mean diameter \bar{R}_s and polydispersity σ_s is consequently reduced to seeking values of $\phi_s, \phi_f, \bar{R}_f$, and σ_f which satisfy the equilibrium conditions given in Eq. (26) as closely as possible. Although it is possible to search for an approximate solution which minimizes, for example, the weighted chemical potential difference at *all* R here we choose a simpler option. We reduce the infinite set of equilibrium conditions to four by requiring equality of chemical potential at just three diameters (R_1, R_2, R_3). Since the majority of the particles have diameters in the range from $\bar{R}(1 - \sigma)$ to $\bar{R}(1 + \sigma)$ we choose the three diameters as

$$R_1 = \frac{\bar{R}_s}{1 - \Delta},$$

$$R_2 = \bar{R}_s, \quad (28)$$

$$R_3 = \frac{\bar{R}_s}{1 + \Delta},$$

where $\Delta^2 = \sigma_s^2 / (1 + \sigma_s^2)$. The equilibrium conditions

$$P_s = P_f, \quad (29a)$$

$$\mu_s(R_1) = \mu_f(R_1), \quad (29b)$$

$$\mu_s(R_2) = \mu_f(R_2), \quad (29c)$$

$$\mu_s(R_3) = \mu_f(R_3), \quad (29d)$$

are solved numerically by using the equality of pressure in the two phases, Eq. (29a), to eliminate the fluid polydispersity σ_f from the set of variables. The remaining three nonlinear equations of chemical equilibrium are solved variationally by minimizing the function \mathcal{F}

$$\mathcal{F}(\phi_s, \phi_f, \bar{R}_f) = (\mu_s(R_1) - \mu_f(R_1))^2 + (\mu_s(R_2) - \mu_f(R_2))^2 + (\mu_s(R_3) - \mu_f(R_3))^2, \quad (30)$$

using a conjugate-gradient algorithm. Coexistence of two phases demands that $\mathcal{F} = 0$.

IV. RESULTS

We have calculated the fluid–solid coexistence boundaries in the polydisperse hard-sphere system as a function of polydispersity. Both coexisting fluid and crystal phases have a Schultz distribution of diameters. Figure 5 shows the volume fractions of the two coexisting phases as a function of the polydispersity of the diameter distribution in the solid, σ_s . As might be anticipated from the discussion in Sec. II B the principle effect of increasing polydispersity is to shift the coexisting fluid density to higher values. The volume fraction of the coexisting solid phase does also increase but at a

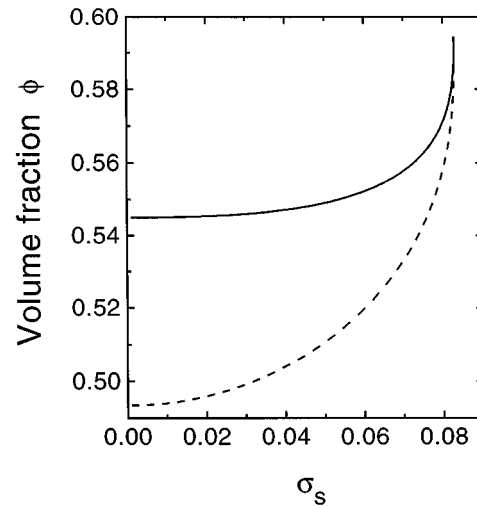


FIG. 5. The volume fraction of coexisting polydisperse crystal (solid) and fluid (dashed) as a function of the polydispersity of the solid phase σ_s .

much lower rate. Consequently with increasing polydispersity the fluid density approaches the solid density. This is most readily seen in Fig. 6 where the ratio $(\phi_s - \phi_f) / \phi_f$ is plotted as a function of σ_s . The most remarkable feature of this figure is that as the solid polydispersity approaches a terminal value of about $\sigma_s^* = 0.0829$ the volume fractions of the two coexisting phases appear to converge. Beyond this terminal value for the solid polydispersity no coexisting solution could be found. Consequently for $\sigma_s > \sigma_s^*$, the polydisperse fluid phase remains the thermodynamically stable phase, within the current model, at all densities.

The value found here for the terminal polydispersity σ_s^* , above which a polydisperse crystal is not stable, is in reasonably close agreement with previous estimates of σ_s^* which lie in the range of 5%–12%. The density functional calculations of Barrat and Hansen⁹ find a value of 6%–7% while McRae and Haymet predict¹⁰ $\sigma_s^* \sim 5\%$. The computer

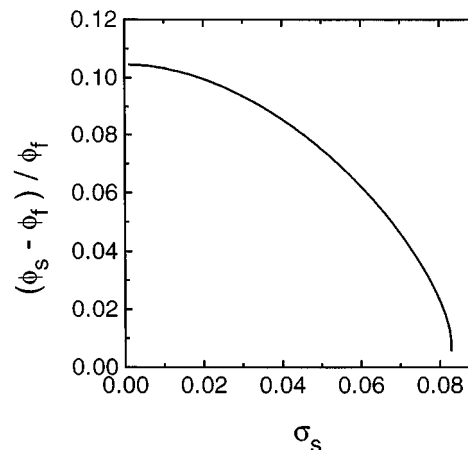


FIG. 6. Relative difference in volume fraction at coexistence as a function of the solid polydispersity σ_s .

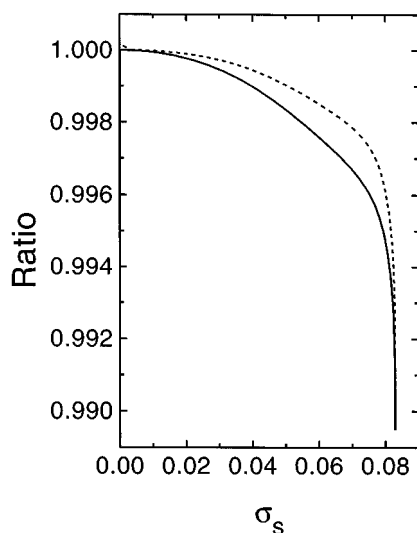


FIG. 7. The ratio of the mean diameters and the polydispersities in the coexisting phases as a function of the solid polydispersity σ_s . The solid line is the ratio \bar{R}_f/\bar{R}_s and the dashed line σ_f/σ_s .

simulations of Bolhuis and Kofke¹¹ find a terminal polydispersity of 5.7% for the solid and 11.8% for the fluid.

In the current calculations the diameter distributions in the fluid and solid phases are, in principle, different. However, we find that the differences between the two distributions are rather small. This is illustrated in Fig. 7 where the ratio (\bar{R}_f/\bar{R}_s) of the mean diameters of the fluid and solid phases are plotted together with the polydispersity ratio (σ_f/σ_s). The average diameter in the fluid is always smaller and is slightly more narrowly distributed than in the coexisting solid. While the effect is more pronounced as the terminal polydispersity is approached the shift in the mean diameter and polydispersity is small, being 1% or less of the solid values. The differences between the diameter distributions in coexisting phases is most readily appreciated from Fig. 8. Here the distributions are plotted for the fluid and solid phases at the terminal polydispersity.

The observation of a small difference in the diameter distributions of the polydisperse fluid and solid is in marked contrast to the simulation results described recently by Bolhuis and Kofke.¹¹ This study found substantial partitioning between the two coexisting phases with the fluid phase containing a wider distribution of diameters (with a smaller mean size) than the solid. At the terminus, where fractionation was most significant, the fluid polydispersity σ_f was over twice the value of the polydispersity of the coexisting solid phase. In contrast, we find that the polydispersities in the fluid and solid phases are very similar (differing by less than 1%) at all points in the phase diagram. While both studies agree that the smaller spheres should be located in the fluid phase, there are differences in the extent of this fractionation. The results of Bolhuis and Kofke suggest a much greater degree of fractionation at the terminal polydispersity with a mean diameter in the fluid phase of about 95% that found in the solid. Our calculations suggest a much closer

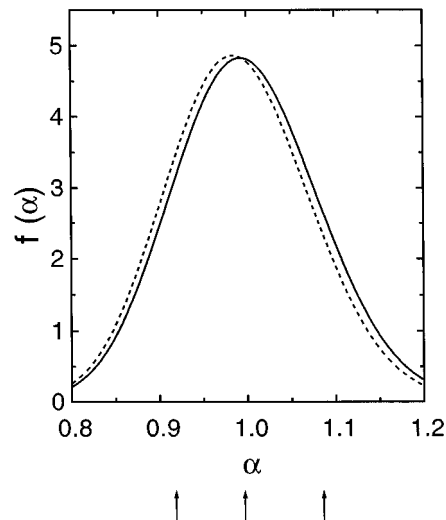


FIG. 8. The diameter distribution in the coexisting crystal (solid) and fluid phases (dashed) evaluated at the terminal polydispersity $\sigma_s=0.0829$. Here α is the scaled diameter R/\bar{R}_s . The arrows label the three specific diameters (R_1, R_2, R_3) where the chemical potential of the solid and fluid phases are equated.

value for the fluid diameter of about 99% of the solid one.

Finally we discuss the accuracy of the solution reported here of the equations of phase equilibria. It is natural to ask if the approximation of matching the chemical potential in the two existing phases at three diameters rather than for all R is valid. Figure 9 illustrates the difference in the chemical potentials $\Delta\mu$ of the two phases as a function of diameter at the terminal polydispersity $\sigma_s^*=0.0829$. Matching the two phases so that $\Delta\mu=0$ at the diameters R_1, R_2 , and R_3 ensures that $\Delta\mu\sim 0$ over the central diameter region where most of the particles lie. Consequently, the approximation

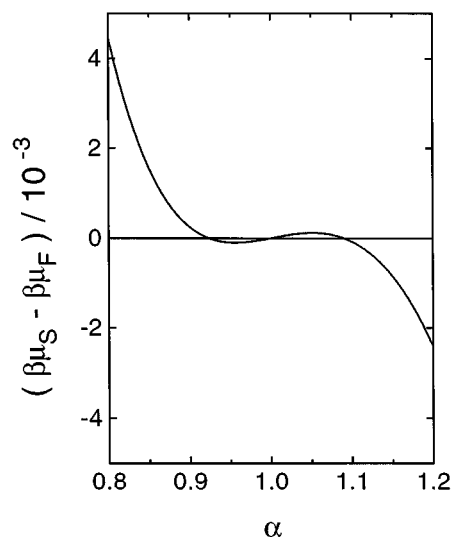


FIG. 9. The chemical potential difference between the coexisting fluid and solid phases, at $\sigma_s=0.0829$, as a function of the scaled particle diameter $\alpha=R/\bar{R}_s$ where \bar{R}_s is the mean diameter in the solid.

looks good. The error in the approximation is, however, more pronounced in the wings of the distribution. The increase in $\Delta\mu$ at small and large α demonstrates that, at thermodynamic equilibrium, the fluid distribution is not precisely Schultz in form. We can gain some idea of the change required in the diameter distribution to achieve full equilibrium by recognizing that, to first order, the effect of changing the diameter distribution is to alter only the ideal term [$\beta\mu^{\text{id}}(\alpha) = \ln \rho\Lambda^3(\alpha)f(\alpha)$]. The excess contribution is a function of the moments of the diameter distribution and is accordingly less sensitive to the details of the distribution. Consequently, a first approximation to the equilibrium fluid distribution, $f^1(\alpha)$, will be

$$f^1(\alpha) = f^0(\alpha) \exp(\beta\Delta\mu) \quad (31)$$

where f^0 is the Schultz-diameter distribution. For the values plotted in Fig. 8 the subsequent change in the distribution from the Schultz form is sufficiently small that the two distributions cannot be distinguished graphically. The approximation of solving the equilibria at just three diameters therefore seems to provide a very good estimate of the phase diagram while affording a significant reduction in computational effort.

V. CONCLUSIONS

In summary we have proposed a simple mean-field description of the effects of polydispersity in hard spheres mixtures. This approach allows the excess thermodynamic properties of a polydisperse mixture to be calculated from a knowledge of the properties of an equivalent binary mixture. In the case of fluid phases our approach is equivalent to scaled particle theory. Comparison with simulation data demonstrates the essential accuracy of the proposed mean-field approximation.

We have used this procedure to calculate the effect of polydispersity on the fluid–solid coexistence of hard spheres. Our results are broadly in line with previous results.^{8–10} We predict that the fluid–solid coexistence densities increase with increasing polydispersity up to a terminal value of the polydispersity of $\sigma_s^* = 0.083$. Above this polydispersity the fluid phase is stable at all densities and no fluid–solid coexistence could be found. The most significant difference from the recent simulations reported by Bolhuis and Kofke¹¹ is in our prediction of a much more limited fractionation between the two coexisting phases. We find an appreciably smaller

difference in the mean diameter and polydispersity in the two coexisting phases as compared with simulation. It is unclear if this discrepancy reflects the neglect of correlations in our simple mean-field picture or is a consequence of the imposed linear chemical potential distribution used in the simulations.

Finally the broad level of agreement observed with other more sophisticated theoretical approaches suggests that the present mean-field treatment provides a simple, yet qualitatively correct, treatment of polydispersity. It therefore is a natural framework for a systematic study of the consequences of polydispersity in a broad range of colloidal phase transitions. More work along these lines is in progress.

ACKNOWLEDGMENTS

This work is supported in part by the Engineering and Physical Sciences Research Council. The author would like to thank Professor P.N. Pusey and Dr. P. Bolhuis for many fruitful discussions.

- ¹W. B. Russel, D. A. Saville, and W. R. Schowalter, *Colloidal Dispersions* (Cambridge U.P., Cambridge, 1989).
- ²M. Baus, L. F. Rull, and J.-P. Ryckaert, *Observation, Prediction and Simulation of Phase Transitions in Complex Fluids* (Kluwer, Dordrecht, 1995).
- ³W. Poon, P. N. Pusey, and H. N. W. Lekkerkerker, *Phys. World* **9**, 27 (1996).
- ⁴P. N. Pusey and W. van Meegen, *Nature* **320**, 340 (1986).
- ⁵P. Bartlett, R. H. Ottewill, and P. N. Pusey, *Phys. Rev. Lett.* **68**, 3801 (1992).
- ⁶W. C. K. Poon *et al.*, *J. Phys. II* **3**, 1075 (1993).
- ⁷A. Imhof and J. K. G. Dhont, *Phys. Rev. Lett.* **75**, 1662 (1995).
- ⁸E. Dickinson and R. Parker, *J. Phys. Lett.* **46**, L (1985).
- ⁹J. L. Barrat and J. P. Hansen, *J. Phys. France* **47**, 1547 (1986).
- ¹⁰R. McRae and A. D. J. Haymet, *J. Chem. Phys.* **88**, 1114 (1988).
- ¹¹P. G. Bolhuis and D. A. Kofke, *Phys. Rev. E* **54**, 634 (1996).
- ¹²H. Reiss, H. L. Frisch, and J. L. Lebowitz, *J. Chem. Phys.* **31**, 369 (1959).
- ¹³J. L. Lebowitz, E. Helfand, and E. Praestgaard, *J. Chem. Phys.* **43**, 774 (1965).
- ¹⁴B. Widom, *J. Chem. Phys.* **38**, 2808 (1963).
- ¹⁵R. C. Tolman, *J. Chem. Phys.* **16**, 758 (1948).
- ¹⁶J.-P. Hansen and I. R. McDonald, *Theory of Simple Liquids*, 1st ed. (Academic, London, 1976).
- ¹⁷J. J. Salacuse and G. Stell, *J. Chem. Phys.* **77**, 3714 (1982).
- ¹⁸W. G. T. Kranendonk and D. Frenkel, *Mol. Phys.* **72**, 679 (1991).
- ¹⁹W. G. T. Kranendonk and D. Frenkel, *Mol. Phys.* **72**, 699 (1991).
- ²⁰W. G. T. Kranendonk and D. Frenkel, *Mol. Phys.* **72**, 715 (1991).
- ²¹G. A. Mansoori, N. F. Carnahan, K. E. Starling, and T. W. Leland, *J. Chem. Phys.* **54**, 1523 (1971).
- ²²J. L. Lebowitz and J. S. Rowlinson, *J. Chem. Phys.* **41**, 133 (1964).
- ²³Here for simplicity we consider only the possibility of equilibrium between two polydisperse phases. We ignore the possibility that a polydisperse fluid might coexist with two or more solid phases.